

## INFLUENCE OF CYCLIC SORPTION ON WOOD ULTRASTRUCTURE

Wiesław Olek,<sup>a,\*</sup> and Jan T. Bonarski<sup>b</sup>

Desorption and adsorption cycles result in dimensional changes of wood. The shrinkage and swelling of wood components are accompanied by the forming and breaking of bonds at sorption sites of water molecules. These processes may lead to some reorganization of the wood ultrastructure. The traditionally applied crystallographic descriptors, i.e. the mean microfibril angle and crystallinity, are unable to quantify such ultrastructural changes. The crystallographic texture analysis was performed to account for the reorganization of wood ultrastructure during the cyclic sorption. The Orientation Distribution Function (ODF) was separately calculated for the selected sorption cycles. Inverse pole figures, texture index, crystalline volume fraction, and integrated skeleton lines of the ODF made a set of crystallographic descriptors used to study the ultrastructural changes within this study. The registered reorganization of the ultrastructure was manifested in changes of the intensities of the individual texture components, including the disappearance of some components. However, the texture index, being the global measure of the crystallographic texture, was practically constant during the cycling sorption.

*Keywords:* Crystallographic texture; X-ray diffraction; Birch wood (*Betula pendula* Roth.)

*Contact information:* a: Faculty of Wood Technology, Poznań University of Life Sciences, Wojska Polskiego 38/42, 60-627 Poznań, Poland; b: Institute of Metallurgy and Materials Science, Polish Academy of Sciences, Reymonta 25, 30-059 Kraków, Poland; \*Corresponding author: olek@up.poznan.pl

### INTRODUCTION

Wood products during their typical use are exposed to natural cyclic variation of moist air parameters, i.e. periodic changes of air temperature and relative humidity. The variation has a daily and seasonal character and induces cyclic changes in moisture content and dimensions of the products. However, the moisture content changes depend, among other things, on the hysteresis of the bound water sorption. The hysteresis is usually explained by changes in the accessibility of sorption sites during desorption and adsorption (Avramidis 1997; Siau 1995; Walker 2006). When bound water is removed from wood during desorption, the constituents of cell walls are brought close enough together to create new bonds between polar groups, i.e. sorption sites. During the inverse process of adsorption, some of the newly formed bonds cannot be broken until the full saturation is obtained. This results in the reduction of available sorption sites and therefore, equilibrium moisture content values during adsorption, with water molecules displacing chains of wood polymers and breaking some already linked sorption sites.

The additional effect of the sorption hysteresis is a possible reduction of equilibrium moisture content as a result of cyclic changes in the air relative humidity (Siau 1995; Skaar 1988).

The long-lasting exposure of wood products to moist air can cause some improvement of wood properties, of which the most prominent is dimensional stability. It is believed that the improvement is related to the alteration of sorption properties, which may be caused by changes in wood's ultrastructure. Unfortunately, the existing investigations have reported inconsistent results relative to the changes in properties. Esteban et al. (2005) performed accelerated ageing of different softwood and hardwood species. Distinct reductions of moisture content values of wood, after ageing, were found for the air relative humidity values close to saturation. Meanwhile, Wu and Ren (2000) did not find differences in sorption isotherms of oriented strand board for subsequent cycles of the air relative humidity variation. However, sorption sites are less available in oriented strand board as compared to solid wood. This is due to the influence of resin content as well as heat and pressure during manufacturing processes. Therefore, the hygroscopic properties of wood-based panels should not be directly compared with those of solid wood. Esteban et al. (2006) compared properties of new and over 200 years old Scots pine wood, concluding that the amorphous zone content of the old wood was higher. The same species was used for determining differences in sorption isotherms, isosteric heat of sorption, and heat of wetting (Esteban et al. 2008). Significant differences of the properties were found for new and old pine wood. Unfortunately, the changes of the thermodynamic properties were not related to ultrastructure changes.

The ultrastructural organization of wood is usually characterized by the mean microfibril angle (e.g. Donaldson 2008; Gierlinger et al. 2010; Lichtenegger et al. 1999). However, due to the helical spatial organization of microfibrils in cell walls, as well as simplifications required for implementing mathematical procedures to determine the mean microfibril angle (e.g. Ogurreck and Müller 2011), the angle alone is not enough to characterize the possible changes of wood ultrastructure that are induced by the cyclic sorption. That disadvantage can be overcome by the analysis of the crystallographic texture. Bonarski and Olek (2006a), as well as Olek and Bonarski (2006), applied the texture function, i.e. the Orientation Distribution Function (ODF), for analyzing materials with monoclinic symmetry. The proposed approach depicted the 3-D ultrastructure of the crystallographically ordered areas of the material. The quantitative analysis of the ultrastructure consisted, among others, of determining complete and inverse pole figures. Recently, the concept of the crystalline volume fraction was proposed in order to increase the accuracy of quantification of crystallographically ordered areas in wood as compared to traditionally used crystallinity or crystallinity index (Bonarski and Olek 2011).

Our previous study (Bonarski and Olek 2006b) presented preliminary results of the influence of the moist air parameters variation on changes of wood ultrastructure. The objective of the present paper is to apply the quantitative texture analysis (i.e. changes of identified dominant texture components, texture index, and crystalline volume fraction) to describe the relation between the ultrastructural properties and wood moisture content changes induced by cycling variation of the air relative humidity.

## MATERIAL AND METHODS

Mature normal birch wood (*Betula pendula* Roth.) was subjected to cycling water sorption by exposure to atmospheres having differing levels of humidity. The material was obtained from a mature tree fallen in Western Poland. Wood discs were cut from the tree at breast height and immediately prevented from uncontrolled water loss. Stripes of green wood were cut from the discs, carefully air-dried below the fiber saturation point (FSP), and next equilibrated to moisture content of ca. 10%. The samples in the shape of rectangular prisms were cut from the equilibrated wood. The thickness of the samples was equal to ca. 6 mm, which corresponded to the radial anatomical direction. The two other dimensions of the samples were 15 and 20 mm. The radial plane of the samples was exposed to X-ray diffraction experiments.

The cycling sorption experiments were made using the desiccator method. The aim of the sorption experiments was to induce a wide range of variation of bound water content in wood. The samples were alternately placed in desiccators containing either dehydrated phosphorus pentoxide or distilled water. This allowed us to obtain two different levels of air relative humidity inside the desiccators, i.e. close to the dry state and saturation. A single sorption cycle consisted of desorption and adsorption phases. The duration of samples staying in each desiccator was at least three days (i.e. the minimum duration of a single sorption cycle was six days). Therefore, the samples achieved bound water contents nearing the dry state and the FSP, respectively. The temperature within the experimental set-up, containing the desiccators, was controlled at the constant level of  $26\pm 0.5^{\circ}\text{C}$ . The total number of the full desorption and adsorption cycles performed in the experiments was equal to 113.

The samples were subjected to X-ray diffraction experiments, which were performed for the following sorption cycles: 0<sup>th</sup> (initial stage of the sorption experiment), 32<sup>nd</sup>, 50<sup>th</sup>, 75<sup>th</sup>, 93<sup>rd</sup>, and 113<sup>th</sup>. The X-ray diffraction pattern was used to select reflections for which the pole figures were registered. The X-ray diffraction experiments were done in an air-conditioned laboratory at the temperature of  $22^{\circ}\text{C}$  and an air relative humidity of 50%. The Schulz back-reflection technique was applied (Schulz 1949). The measurements were performed with a Philips X'Pert system equipped with a texture goniometer ATC-3, which enabled the same positioning of the samples for the subsequent X-ray diffraction experiments corresponding to the selected sorption cycles. Each X-ray diffraction experiment was performed for a large volume of the investigated material, ca.  $0.8\text{ mm}^3$ . Therefore, the measurements delivered averaged characteristics of the ultrastructure as compared to the traditional X-ray diffraction methods applied for investigating wood ultrastructure. Additionally, during a single X-ray diffraction experiment, 642 individual diffraction patterns were registered in order to increase reliability of the performed analysis. The incomplete pole figures of the (101), (001), and (010) planes were measured. The unit cell of cellulose I $\beta$  is described by the monoclinic crystal system (e.g. Zugenmaier 2008). Within the present study the set of Miller's indices corresponding to the sequence of diffraction reflections for the (101), (002), and (040) planes of the reference monoclinic lattice was applied according to "International tables for crystallography" (Burzlaff and Zimmermann 2006), which provided the most current recommendations for indexing crystallographic lattices. After performing the defocusing

correction, experimental data were processed using the ADC method in order to calculate the 3D ODF, being the three-dimensional representation of the texture function (Bunge 1982). The ODF calculations were performed according to the procedure implementing the ODF to materials of the monoclinic lattice symmetry (Bonarski and Olek 2006a; Olek and Bonarski 2006).

A set of crystallographic descriptors was proposed to study the ultrastructural changes. The descriptors consisted of inverse pole figures, texture index, crystalline volume fraction, and integrated skeleton lines of the ODF. The crystalline volume fraction was originally proposed by Bonarski and Olek (2011) along with a procedure for quantifying fractions of the ordered and amorphous areas in wood. The developed procedure was called the Global Crystalline-Amorphous Signal (GC-AS) method. It accounted for a specific space arrangement of bio-composites. The GC-AS method made it possible to describe the intensities of diffraction reflections that were not disturbed due to a preferred orientation of the wood phases. Moreover, the complete intensities of crystalline and amorphous phases were used in the analysis. This allowed taking into consideration partially ordered wood constituents, i.e. non-crystalline cellulose, hemicelluloses, and lignin (e.g. Stevanic and Salmén 2009), which contributed to the diffraction signal. The method was a more adequate measure of the quantity of the ordered and amorphous areas, as it accounted for the influence of the preferred crystallographic orientation of wood texture on the ultrastructural organization.

The ODFs were determined for six cycles of the sorption experiment. The texture functions obtained in this way were used to derive different crystallographic characteristics of the investigated material in order to characterize the ultrastructural changes caused by cycling variation of the air relative humidity.

## RESULTS AND DISCUSSION

The most obvious descriptors of crystallographic orientations are complete pole figures, which are stereographic projections representing the statistical average distributions of poles of specific crystalline planes in a polycrystalline material. Therefore, the sets of complete pole figures, (101), (001), and (010), were derived from the corresponding ODFs for all the analyzed cycles of the sorption experiment. The complete pole figures represent a 2D projection of a selected  $\{hkl\}$ -lattice plane, which is identical to the examined surface of the material. Figure 1 presents an example of the complete (001) pole figure as obtained for all investigated sorption cycles. The obtained complete pole figures showed the essential differences in the distributions of the basic planes of the crystallographic system of the organized areas of birch wood for the subsequent cycles of the sorption process. Regarding the initial stage of the sorption process, as the reference for the texture analysis, the subsequent stages caused essential changes in the density distribution of the (001) poles concentrated closely to the transverse (*TR*) plane of the examined wood (Fig. 1). The changes consisted of decomposing the area with maximal pole density identified in the central part of the (001) pole figure into two subareas of the orientations. The intensities of the misoriented subareas corresponded to the crystalline volume fraction increasing up to the 75<sup>th</sup> cycle of

sorption (Fig. 4). However, the misorientation identified in the complete pole figures was increasing during the whole experiment of cycling sorption and obtained its maximum at the 93<sup>rd</sup> cycle (Fig. 1).

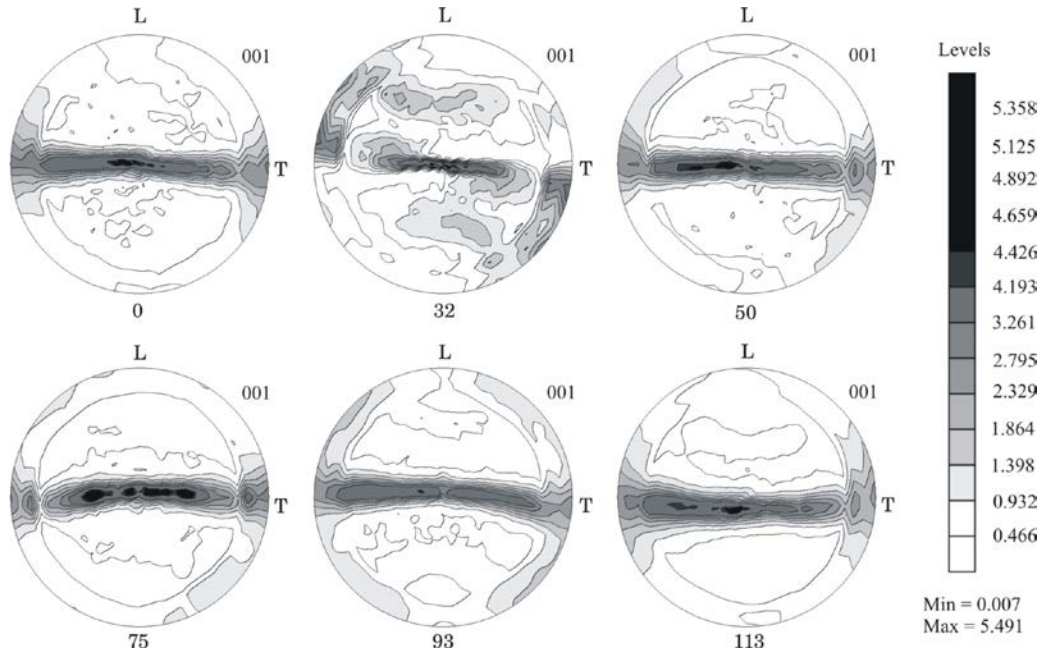


**Fig. 1.** Complete pole figures (001) calculated from the ODFs for the 0<sup>th</sup> (the initial stage of sorption), 32<sup>nd</sup>, 50<sup>th</sup>, 75<sup>th</sup>, 93<sup>rd</sup>, and 113<sup>th</sup> sorption cycles. *L* and *T* are the longitudinal and tangential directions of the reference coordinate system (the maximum pole density identified in the central part of the figures and decomposed into two misoriented subareas).

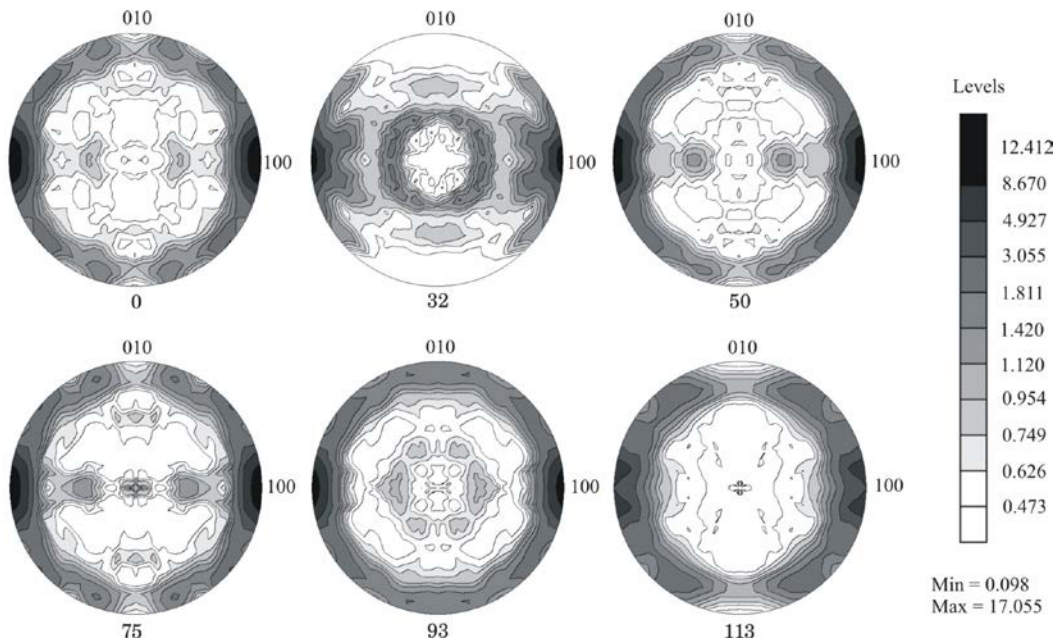


**Fig. 2.** Inverse pole figures of the *L* direction - calculated from the ODFs for the 0<sup>th</sup> (the initial stage of sorption), 32<sup>nd</sup>, 50<sup>th</sup>, 75<sup>th</sup>, 93<sup>rd</sup>, and 113<sup>th</sup> sorption cycles. 010 and 100 are directions of the cellulose crystal lattice coordinate system.

Inverse pole figures are other descriptors of crystallographic orientations derived from the ODFs. An inverse pole figure is usually defined as an angular distribution of a selected direction of the investigated material with respect to the ordered areas system (e.g. Engler and Randle 2010). Therefore, inverse pole figures represent a 2D projection of a selected anatomical direction of wood. The obtained inverse pole figures have special importance in interpreting changes of the spatial arrangement of the ordered areas of wood. Figure 2 presents a set of inverse pole figures of the longitudinal anatomical direction, ( $L$ ), obtained for the selected sorption cycles. The already identified changes of the spatial orientation of the ordered areas were also found in the inverse pole figures. In this instance the descriptor changes in the spatial orientation are related to crystallographic elementary cell of the monoclinic symmetry. Unlike the complete pole figures, the inverse pole figures have distinct monoclinic (twofold) symmetry. This is due to their representation in the crystal lattice coordinate system, here in the system of the 100 and 010 directions.

It is evident from the figures that a distinct reorientation of the (001) planes of the ordered areas developed towards the transverse ( $TR$ ) plane. Moreover, a tendency of rotating the ordered areas from the position in which the  $\langle 101 \rangle$  lattice direction was parallel to the  $L$  direction towards the  $\langle 100 \rangle$  direction was observed. The tendency was also manifested in grouping the intensities of the inverse pole figures into two subregions, i.e. central and peripheral ones. The grouping process was the most distinct between the 32<sup>nd</sup> and 93<sup>rd</sup> cycles (Fig. 2). The changes were accompanied by other rotations characterized by high spread of orientations. The changes reflected in the mean microfibril angle distribution, i.e. the observed values of the angle, were grouped in a few ranges. Nevertheless, the detailed analysis of the distribution is beyond the scope of this paper.

The already performed analysis of the complete and inverse pole figures revealed local changes in the texture components. However, the global development of the crystallographic texture is often quantified with the use of the texture index ( $J$ ) being the overall measure of the texture sharpness. The texture index is given by the following integral (Bunge 1982),

$$J = \oint [f(g)]^2 dg \quad (1)$$

where  $f(g)$  is the texture function (here ODF), and  $g$  is the crystallographic orientation. Such a definition of the texture index implied the following range of the index values  $[1, \infty)$ . Therefore, Bonarski (2006) introduced the normalized texture index ( $J_n$ ) defined as

$$J_n = \frac{J - 1}{J + 1} \quad (2)$$

with its values ranging in the interval of  $[0, 1]$ , which was more convenient to quantify the development of the texture. The normalized texture index was calculated for the six-sorption cycles of the investigated birch wood. The obtained results for  $J_n$  are presented

in Fig. 3. It is evident from the plot that the changes in the texture index values were practically insignificant during the evolution of the sorption experiment. It can be interpreted that the local changes of the texture, i.e. the already observed changes of particular texture components, had no essential influence on the global texture sharpness, which remained practically constant. Moreover, the insignificant changes of the texture index ( $J_n$ ) might indicate that wood ultrastructure is characterized by the relatively stable degree of texturization. The texture index did not reveal changes in individual texture components. The changes of the components were qualitative (Miller indices) as well as quantitative (intensities). Therefore, the spatial arrangement of the ordered areas was complex and was observed with the use of the ODFs skeleton lines (Fig. 5). The most intensive changes were observed for the  $\{100\}\langle 010\rangle$  component.

The ultrastructural organization of wood is also frequently characterized by crystallinity, which is used to quantify contents of accessible and non-accessible areas of cellulose for water sorption, chemical modification, as well as biological decay (Rowell et al. 2005). Therefore, the crystallinity should be of special importance when characterizing possible additional reorganization of wood ultrastructure due to cycling sorption. Thygesen et al. (2005) reviewed and criticized the standard X-ray diffraction methods for the crystallinity determination. The concept of the global diffraction signal was applied in the present study, and newly developed crystalline volume fraction was used to quantify the ultrastructural organization of wood (Bonarski and Olek 2011). The values of the crystalline volume fraction were separately calculated for the six cycles of the sorption experiment (Fig. 4).

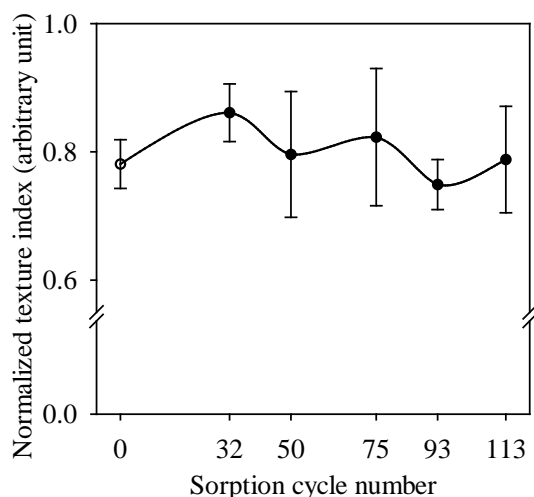
A distinct and gradual increase of the crystalline volume fraction was observed as compared to the initial phase of the cycling sorption. However, after the 75<sup>th</sup> sorption cycle, the crystalline volume fraction was practically constant for the continued cycling sorption. The increase can be attributed to possible reorganization of wood constituents due to displacing some polymers and creation of new bonds between polar groups (i.e. sorption sites) during water desorption. It may be supposed that at least parts of the new bonds are not broken during adsorption. Such reorganization could be attributed to amorphous cellulose and hemicelluloses.

Figure 5 shows the integrated skeleton lines representing the maximum values of the ODF being described in the orientation space of Euler angles (Bunge 1982). The skeleton lines had to be shown for a selected dimension of the orientation space, e.g. for  $\varphi_1$  angle. The individual values of the skeleton lines were obtained as the integrals over the elementary ODFs cells (i.e.  $\Delta\varphi_1$  by  $\Delta\Phi$  by  $\Delta\varphi_2$ ), which surrounded the maximum value in the related ODFs areas. The skeleton lines were characterized by local maxima corresponding to the orientations (i.e. texture components) dominating in the texture. The following texture components were identified for investigated birch wood, i.e.  $\{100\}\langle 010\rangle$ ,  $\{112\}\langle 11-1\rangle$ ,  $\{2-12\}\langle -1-20\rangle$ , and  $\{0-10\}\langle 10-1\rangle$  (Fig. 5). The presence of the dominating  $\{100\}\langle 010\rangle$  component in the texture indicates that the distinct part of the microfibrils is oriented almost parallel to the *LT* anatomical plane of wood (the 10° spreading is considered here). Simultaneously, the longitudinal axes of the microfibrils are also almost parallel to the longitudinal anatomical direction of wood. The other minor texture components indicate parallel alignment of their identified lattice

planes and crystallographic directions to the *LT* anatomical plane and longitudinal anatomical direction, respectively.

The orientation of the microfibrils, revealed by the ODF, is precisely determined by the identified texture components, which also describe several ranges of the spatial orientation of microfibrils. The orientations can be estimated by traditional methods for the mean microfibril angle determination (e.g. Cave 1997a;b). In the case of the traditional methods, only 2-D sections of the 3-D arrangement of microfibrils are observed. As was depicted in Fig. 5, the  $\{100\}\langle 010\rangle$ -texture component dominated in each analyzed sorption cycle in spite of the changes of its intensity.

The component changes are accompanied by fluctuations of intensities of other components reflecting transformations of the spatial ultrastructure during the cycling sorption. The observed reorganization consisted of the increasing and decreasing (including disappearance) of the intensities of the individual texture components. These changes were not reflected in the texture index ( $J_n$ ) values, which remained almost constant (Fig. 3).



**Fig. 3.** Changes of the normalized texture index ( $J_n$ ) for the selected sorption cycles (error bars represent spreading of the  $J_n$  values resulted from the ODF iteration procedure)

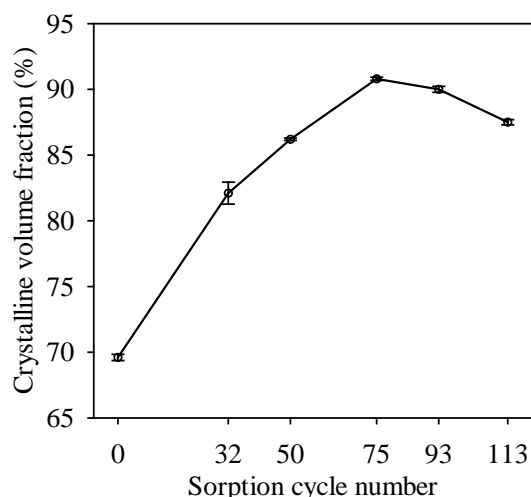


**Fig. 4.** Evolution of the crystalline volume fraction for the selected sorption cycles (error bars represent the uncertainty of the crystalline volume fraction determined with the total derivative method)

The observed changes of wood ultrastructure are related to all wood components. However, the scope of the changes is different for cellulose, hemicelluloses, and lignin. The primary changes were identified for the most oriented areas, which were assigned to crystalline cellulose. The dynamics of the changes was already found when analyzing the complete pole figures (Fig. 1) as well as inverse pole figures of the longitudinal direction (Fig. 2). However, the reorganization of cellulose was most clearly visible when analyzing the integrated skeleton lines of the ODFs (Fig. 5). The changes were identified not only for the dominating  $\{100\}\langle 010\rangle$  orientation but also for minor orientations, which could be related to less organized wood components (i.e. hemicelluloses) and to



some extent to lignin. It was found that the minor orientations were characterized by fluctuations in their intensities.

The quantitative ultrastructural changes of less organized wood components (i.e. hemicelluloses and lignin) were also found when analyzing the results of crystalline volume fraction, which was gradually and considerably increasing up to the 75<sup>th</sup> sorption cycle. The increase as well as relatively high values of crystalline volume fraction could be related to the additional crystallographical organization of the areas, which were usually defined as amorphous (lignin) or low organized (hemicelluloses). The contents of less organized wood components were included in the concept of the crystalline volume fraction because of the application of the CG-AS method, in which the integrated intensities of the global diffraction effects were considered, instead of the maximum intensity alone. Moreover, the reorganization of hemicelluloses and lignin was interrelated to the changes in ultrastructure of cellulose. This was in accordance with the observations reported by Salmén et al. (2012), which related structuring of lignin in the S2 layer to the presence of cellulose being a kind of template for lignin deposition and so mapping its high ultrastructural organization in lignin.

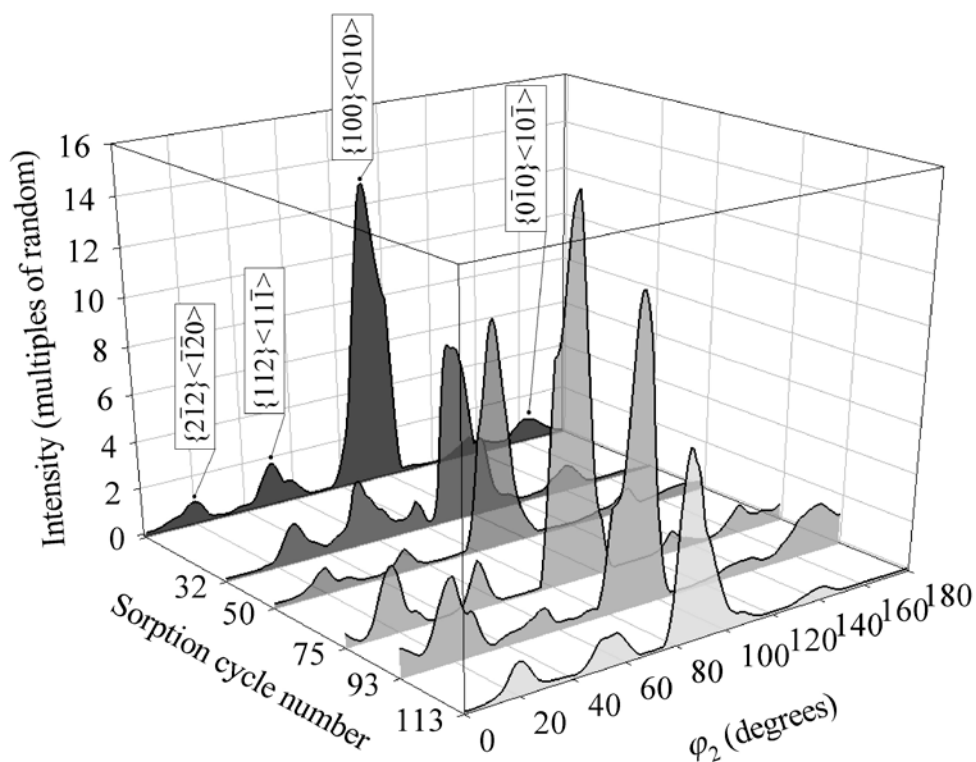


**Fig. 5.** Integrated skeleton lines (intensity vs.  $\varphi_2$ ) of the orientation distribution function in the Euler orientation space depicted separately for the selected sorption cycles

## CONCLUSIONS

1. The cyclic sorption caused reorganization of birch wood ultrastructure. The reorganization consisted of transformation of the texture components. The most intensive

- changes were revealed for the  $\{100\}\langle 010\rangle$  orientation, with its maximum value being attained at the 75th sorption cycle. The changes were accompanied by the maximum of the crystalline volume fraction at the same stage of cyclic sorption.
2. It has been recommended that the changes in wood ultrastructure should be described by the application of the set of crystallographic descriptors consisting of inverse pole figures, texture index, crystalline volume fraction, and integrated skeleton lines of ODFs.
  3. The qualitative analysis of the inverse figures of the  $L$  direction showed that the cyclic sorption caused changes in the spatial distribution and magnitude of the mean microfibril angle into the limited extent only.
  4. The texture index being a measure of the global texture sharpness was an insensitive measure of the ultrastructural changes. Meanwhile, the crystalline volume fraction was used to identify the reorganization attributed to possible creation of new bonds between polar groups of wood constituents.

## REFERENCES CITED

- Avramidis, S. (1997). "The basics of sorption," In: P. Hoffmeyer (ed). *Proceedings of the International Conference of COST Action E8 "Mechanical Performance of Wood and Wood Products"*, 16-17 June 1997, Copenhagen, Denmark: 1-18.
- Bonarski, J. T. (2006). "X-ray texture tomography of near-surface areas," *Prog. Mater. Sci.* 51, 61-149.
- Bonarski, J., and Olek, W. (2006a). "Texture function application for wood ultrastructure description. Part 1. Theory," *Wood Sci. Technol.* 40, 159-171.
- Bonarski, J. T., and Olek, W. (2006b). "Crystallographic texture changes of wood due to air parameter variations," *Z. Kristallogr.* 23, 607-612.
- Bonarski, J. T., and Olek, W. (2011). "Application of the crystalline volume fraction for characterizing the ultrastructural organization of wood," *Cellulose* 18, 223-235.
- Bunge, H. J. (1982). *Texture Analysis in Materials Science*, Butterworths, London.
- Burzlaff, H., and Zimmermann, H. (2006). "Bases, lattices, Bravais lattices and other classifications," In: Th. Hahn (ed). *International Tables for Crystallography*. Volume A: Space-group symmetry, Springer, Berlin, Chapter 9.1: 742-749.
- Cave, I. D. (1997a). "Theory of X-ray measurement of microfibril angle in wood. Part 1. The condition for reflection X-ray diffraction by materials with fibre type symmetry," *Wood Sci. Technol.* 31, 143-152.
- Cave, I. D. (1997b). "Theory of X-ray measurement of microfibril angle in wood. Part 2. The diffraction diagram," *Wood Sci. Technol.* 31, 225-234.
- Donaldson, L. (2008). "Microfibril angle: measurement, variation and relationships - A review," *IAWA J.*, 29, 345-386.
- Engler, O., and Randle, V. (2010). *Introduction to Texture Analysis: Macrotecture, Microtexture, and Orientation Mapping*, 2nd Ed. CRC Press, Boca Raton.
- Esteban, L. G., Fernández, F. G., Guindeo, A., de Palacios, P., and Gril, J. (2006). "Comparison of the hygroscopic behaviour of 205-year-old and recently cut juvenile wood from *Pinus sylvestris* L.," *Ann. Forest Sci.* 63, 309-317.

- Esteban, L. G., Gril, J., de Palacios, P., and Guindeo, A. (2005). "Reduction of wood hygroscopicity and associated dimensional response by repeated humidity cycles," *Ann. Forest Sci.* 62, 275-284.
- Esteban, L. G., de Palacios, P., Fernández, F. G., Guindeo, A., and Cano, N. N. (2008). "Sorption and thermodynamic properties of old and new *Pinus sylvestris* wood," *Wood Fiber Sci.* 40, 111-121.
- Gierlinger, N., Luss, S., König, C., Konnerth, J., Eder, M., and Fratzl, P. (2010). "Cellulose microfibril orientation of *Picea abies* and its variability at the micron-level determined by Raman imaging," *J. Exp. Bot.* 61, 587-595.
- Lichtenegger, H., Reiterer, A., Stanzl-Tschegg, S. E., and Fratzl, P. (1999). "Variation of cellulose microfibril angles in softwoods and hardwoods - A possible strategy of mechanical optimization," *J. Struct. Biol.* 128, 257-269.
- Ogurreck, M., and Müller, M. (2011). "Analytical description of the scattering of cellulose nanocrystals in tracheid wood cells," *J. Appl. Crystallogr.* 43, 256-263.
- Olek, W., and Bonarski, J. (2006). "Texture function application for wood ultrastructure description. Part 2. Application," *Wood Sci. Technol.* 40, 336-349.
- Rowell, R. M., Pettersen, R., Han, J. S., Rowell, J. S., and Tshabalala, M. A. (2005). "Cell wall chemistry," In: R. M. Rowell (ed). *Handbook of Wood Chemistry and Wood Composites*, CRC Press, Boca Raton.
- Salmén, L., Olsson, A.-M., Sevanic, J. S., Simonović, J., and Radotić, K. (2012). "Structural organisation of the wood polymers in the wood fibre structure," *BioResources* 7, 521-532.
- Schulz, L. G. (1949). "A direct method of determining preferred orientation of a flat reflection sample using a Geiger counter X-ray spectrometer," *J. Appl. Phys.* 20, 1030-1033.
- Siau, J. F. (1995). *Wood: Influence of Moisture on Physical Properties*, Virginia Polytechnic Institute and State University, Blacksburg.
- Skaar, C. (1988), *Wood-Water Relations*, Springer, Berlin.
- Stevanic, J. S., and Salmén, L. (2009). "Orientation of the wood polymers in the cell wall of spruce wood fibres," *Holzforschung* 63, 497-503.
- Thygesen, A., Oddershede, J., Lilholt, H., Thomsen, A. B., and Ståhl, K. (2005). "On the determination of crystallinity and cellulose content in plant fibres," *Cellulose* 12, 563-576.
- Walker, J. (2006), "Water in wood," In: J. C. F. Walker (ed). *Primary Wood Processing. Principles and Practice*, 2nd Edition. Springer, Dordrecht.
- Wu, Q., and Ren, Y. (2000). "Characterization of sorption behavior of oriented strandboard under long-term cyclic humidity exposure condition," *Wood Fiber Sci.* 32, 404-418.
- Zugenmaier, P. (2008). *Crystalline Cellulose and Derivatives: Characterization and Structures*, Springer, Berlin.

Article submitted: November 30, 2011; Peer review completed: December 10, 2011;  
Revised version received and accepted: January 30, 2012; Further revisions accepted:  
February 17, 2012; Article published: February 20, 2012.